ADVANCED ENGINEERING MATERIALS

COMMUNICATIONS

DOI: 10.1002/adem.200800072

Porous Titanium by Electro-chemical Dissolution of Steel Space-holders**

By *Peter Jordan Kwok, Scott M. Oppenheimer* and *David C. Dunand**

Among the various methods existing to fabricate porous titanium for structural or biomedical applications,[1] the space-holder approach is particularly useful as it allows a close control of pore size, shape and fraction. In this method, a blend of pure or alloyed titanium powders and space-holder materials are cold-pressed into a preform which is sintered in vacuum. During the early stage of sintering, the space-holder is removed by evaporation or decomposition, creating porosity in the titanium. Space-holders in powder form used to create titanium foams have included carbamide (urea),[2,3] magnesium,[4,5] ammonium hydrogen carbonate[6–8] and polymers.[9,10].

There is considerable interest in creating titanium foams with elongated pores for applications such as filters, heat exchangers and biomedical implants. Elongated pores in titanium have been created by the anisotropic expansion of entrapped argon in solid titanium.[11–13] Using the space-holder method, polymer/titanium preforms were extruded, thus producing, *in-situ,* elongated space-holders.[14] In another recently demonstrated method, the elongated space-holder consists of ice dendrites which are formed *in-situ* by directional solidification of a water/titanium slurry and are sublimated before titanium is densified.[15] Alternatively, if the space-holder can be drawn *ex-situ* into wires, these wires can be incorporated into the titanium powder preform in an initial step, before being removed by evaporation or decomposition during densification. This approach produces pores with regular shapes and has, to our knowledge, been demonstrated in titanium foams only with magnesium wires (180–450 μm in diameter).[4]

Here, we examine steel as a novel space-holder for creating porosity in sintered titanium. This approach differs from the existing methods reviewed above because the steel space-holders are removed after densification by electrochemical dissolution, rather than during or before densification by evaporation or decomposition, as in previous studies. Furthermore, steel is easier to shape in sub-millimeter wires than the Mg wire space-holders used in the only previous study using metallic wires.[4] However, this approach must address the interdiffusion between Ti and Fe expected to occur during densification. Here, we demonstrate the creation of intricate pore shapes replicating faithfully steel space-holders in the shape of both spheres and wires. We also show that Fe-Ti interdiffusion can be inhibited by the *in-situ* formation of a TiC reaction layer, and that, alternatively, if an interdiffusion layer forms, it can be removed by dissolution, resulting in increased porosity.

Experimental Procedures

Preforms with 12.5 mm diameter, consisting of titanium powders containing steel space-holders in the form of wires, spheres and wire meshes, were uniaxially cold-pressed to 350 MPa. Commercially-pure titanium powders (from Atlantic Equipment Engineers, NJ) were sieved to -325 mesh (~ 40 μm size) and exhibited non-spherical shape. Independent chemical analysis showed high oxygen content (0.81 wt.% O) and low other interstitials (0.031 wt.% H and 0.057 wt.% C). Table 1 summarizes details about the steel place-holders, some of which were pack-carburized with activated graphite powder (PTI Process Chemicals) at 960 °C for 1 h. Preforms were sintered under high vacuum (~ 10^{-6} torr) for 12 h at 1050 °C, below the Ti-Fe eutectic temperature of 1085 °C.

Steel was removed from the sintered Ti-Fe composites in an electrolytic cell with a cylindrical titanium sheet acting as the cathode, the sample as the anode, and a 10 vol.% acetic acid aqueous solution fully saturated with NaCl as the electrolyte. Other electrolytes (based on chromic acid, sodium ni-

Table 1: Iron and steel space-holders

Shape	Materials	Diameter	Supplier
Sphere	Low-carbon steel 1010–1020 (0.10–0.20 %C)	1.58 mm	McMaster Carr
Wire	Iron (99.5% pure) (~0.01% C)	250 and 406 mm	ESPI Corp.
Wire	Tempered high-carbon steel (0.80–0.95 %C)	250 and 500 mm	McMaster Carr
Mesh	Mild steel	508 mm (wires), woven with 5.5 wires/cm	McMaster Carr

[*] *P. J. Kwok, Dr. S. M. Oppenheimer, Prof. D. C. Dunand*
Department of Materials Science and Engineering
Northwestern University
Evanston, IL 60208, USA
E-mail: dunand@northwestern.edu

[**] *This research was supported by US National Science Foundation through Grant DMR-0505772.*

trate, oxalic acid, sodium hydroxide, sodium chloride, and ammonium hydroxide) were tested but not used, since they did not perform as well. A 6 V potential was applied across the cell (below the 7 V threshold where titanium dissolution was observed), and a distance of 2–4 cm was maintained between the cathode and the Ti-Fe composite, ensuring a uniform electrical field around the anode. Ultrasonic agitation was imposed on the cell, a method that was previously shown to enhance material removal during micro-electro discharge machining.[16] The temperature of the bath was ~ 35 °C.

One sample containing a single high-carbon wire (500 μm in diameter and ~ 8 mm in length) exposed to dissolution at both its ends, was subjected to dissolution steps with time increments of 30 min, interrupted by drying and weighing, from which the mass of the wire removed was determined. The depth of the two cavities, one formed on each side of the sample by the dissolution of the wire, was calculated from the mass loss and found to be in agreement with direct depth measurements performed by introducing a thinner wire into one of the cavities.

After steel dissolution, samples were cut on a diamond saw, hot-mounted in phenolic resin (which also filled the porosity) and polished with 9 and 0.05 μm alumina suspensions before being micrographed in an optical microscope.

Results and Discussion

Cylindrical Cavities

Figure 1 shows the kinetic of dissolution for a 500 μm diameter high-carbon steel wire, with a length of ~ 8 mm, exposed to the solution at both sides of the titanium billet in which it was embedded. The dissolution rate decreases steadily as the depth of the two opposite cavities increases, because removal of the dissolution products and transport of fresh solution by diffusion and convection becomes more difficult. Nevertheless, a relatively rapid dissolution rate of ~ 1.8 mm/h (0.5 μm/s) was achieved in the first hour. Full dissolution of the wire was completed after about 10 h. with both cavities joining to form a cylindrical channel, with a depth of ~ 8 mm and an aspect ratio of ~ 16, perforating the titanium sample. Thinner wires necessitated longer times to fully dissolve, *e.g.*, a 250 μm diameter carburized iron wires with 7 mm embedded depth (with an aspect ratio of 28, shown in cross-section in Figure 2(a)) was fully removed after about 20 h. Figure 2(b) shows the corresponding cylindrical cavity after dissolution, with some erosion of the sides possibly due to polishing damage of the incompletely-sintered titanium matrix near the cavity edge. Even if the sides of the cavity are not smooth, this roughness may be advantageous for bone anchorage in a bone implant application. The titanium matrix was not fully sintered because of the relatively

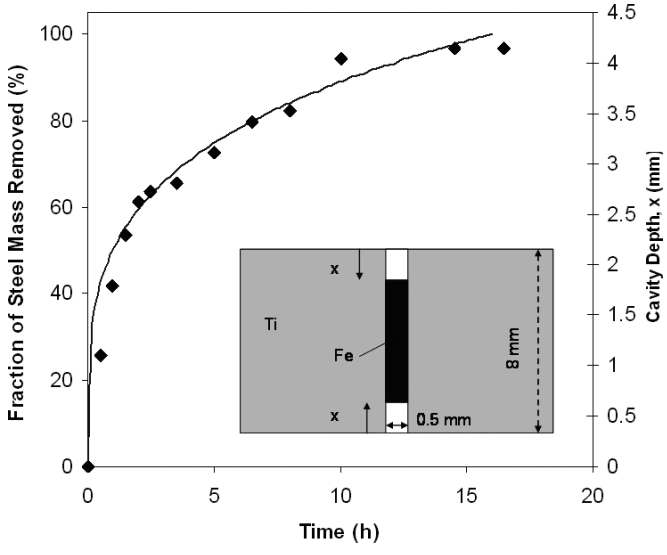

Fig. 1. Kinetic of dissolution for a single 500 μm high-carbon steel wire embedded in titanium. Mass loss was measured and depth was calculated based on an initial wire length of 8 mm.

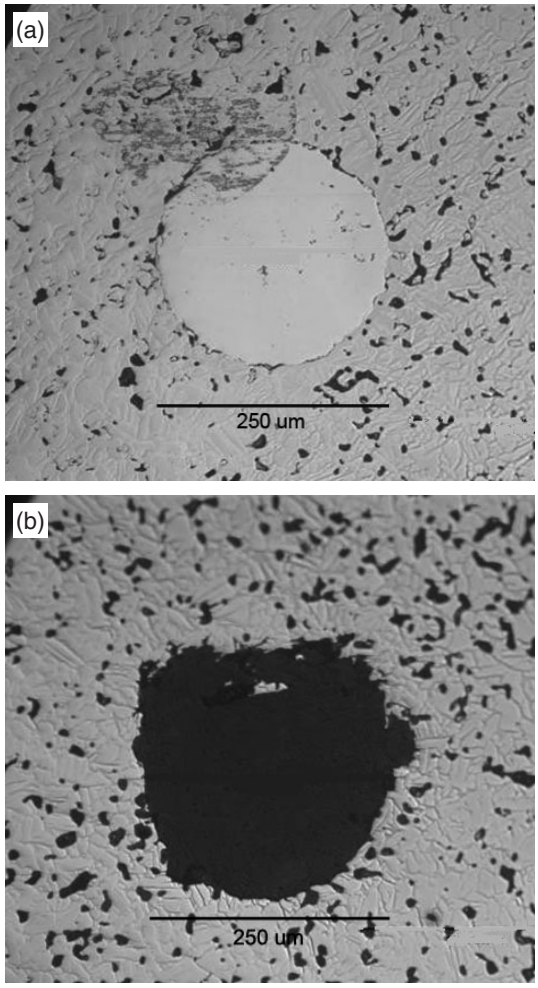

Fig. 2. Radial cross-section of titanium billet containing (a) a 250 μm diameter carburized iron wire and (b) a cylindrical cavity of similar diameter created by dissolution of the wire.

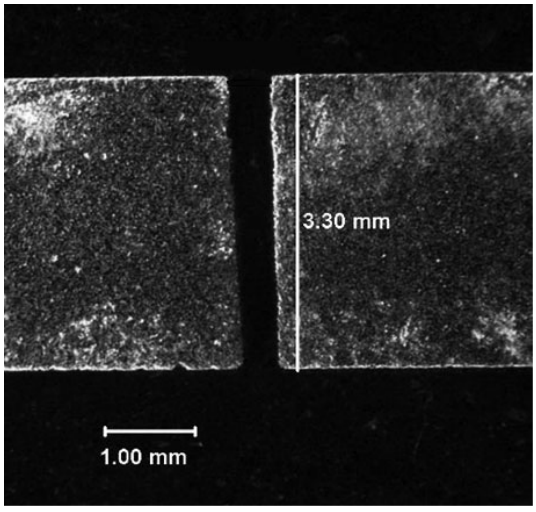

Fig. 3. Longitudinal cross-section of titanium billet showing the first 3.3 mm of a ~ 8 mm deep cylindrical cavity created by dissolution of a 500 μm diameter steel wire (Fig. 1). Original sample surface is at the top of image.

low sintering temperature which could not exceed the Ti-FeTi eutectic temperature.

Figure 3 shows a longitudinal cross-section of half the cylindrical cavity created by dissolution of the high-carbon steel wire with 500 μm diameter whose kinetic data is shown in Figure 1. Here, only the first 3.3 mm of the ~ 8 mm wire are shown. This figure illustrates the excellent edge retention of the cavity near the specimen surface (subjected for the longest time to the acid) and the uniformity of the cavity diameter, demonstrating that titanium did not dissolve during the steel dissolution as a result of cathodic protection.

Prior literature indicates that the presence of carbon in steel reduces inter-diffusion between iron and titanium by the formation of a TiC interfacial layer.[17] In that study, lack of inter-diffusion was detrimental, since it prevented diffusion bonding of the two metals. However, in the present study, interdiffusion may be undesirable, because the iron contamination of the titanium matrix near the wires may result in a brittle region. To test this hypothesis, titanium preforms were sintered with iron wires, with or without prior carburization, and subjected to wire dissolution. As shown in Figures 4(a–b), the carburized wire is dissolved from the titanium matrix and leaves a cylindrical cavity with the same diameter as the wire, indicating that, as for the carburized iron wire shown in Figure 2, titanium dissolution was completely inhibited. By contrast, an uncarburized iron wire with 406 μm diameter resulted, after dissolution, in a cylindrical cavity with twice the diameter of the original wire (Figs. 5(a–b)), indicating that considerable dissolution of the titanium matrix surrounding the wire took place; the titanium volume removed consists of three times the volume of the original steel wire. Interestingly, the shape of the resulting cavity is nearly circular and its radius (400 μm) is close to the sum of the original wire radius (203 μm) and the extent of the diffusion layer, visible as a ~ 150 μm thick shell of coarse,

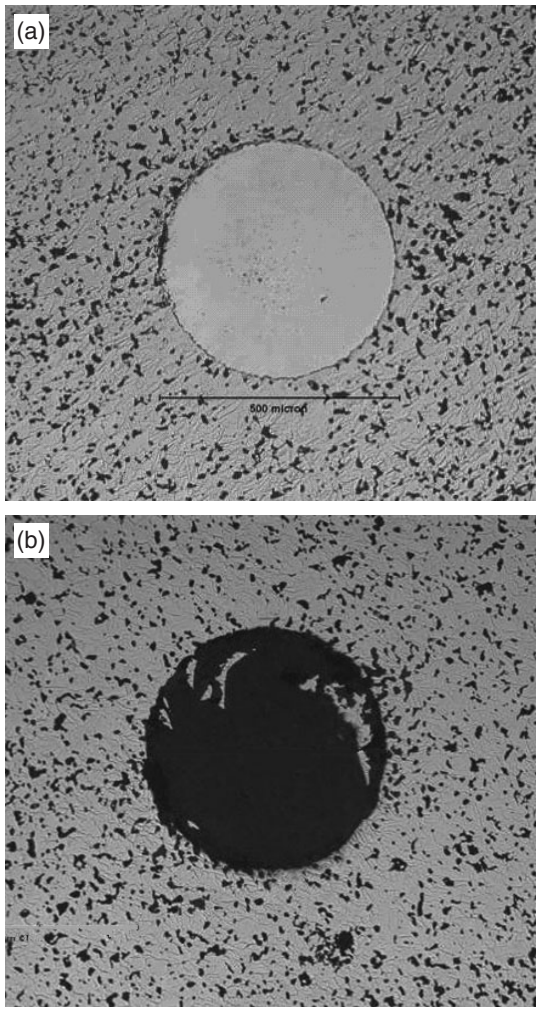

Fig. 4. Radial cross-section of titanium billet containing (a) a 500 μm carburized iron wire and (b) a cylindrical cavity with the same diameter produced by dissolution of the wire (polishing debris are embedded in phenolic resin filling the cavity). Both images have the same magnification.

recrystallized grains surrounding the wire in the etched cross-section of the composite in Figure 6. The diffusion distance of Fe in Ti, estimated from $2(Dt)^{1/2}$ (where D is the inter-diffusion coefficient in the Fe-Ti system[18] and t is the sintering time), is in the range of 10–460 μm for diffusion in the intermetallic $TiFe_2$ phase and the Ti(Fe) solid solution, respectively, confirming that the ~ 150 μm wide shell indeed corresponds to a region with high Fe content. Thus, it appears that the applied voltage was sufficient to dissolve both the steel wire and the surrounding iron-containing titanium shell. This provides an approach to increasing the volume fraction of the cavities well beyond the fraction of steel, while maintaining their circular shapes. Further experiments will determine the Fe concentration in the metal surrounding the cavity in Figure 5(b).

Finally, a titanium sample containing ten layers of carburized steel mesh (consisting of woven 508 μm diameter wires) was sintered. A cross-section of the composite before steel dissolution is shown in Figure 7(a). Another cross-section of

ADVANCED ENGINEERING MATERIALS

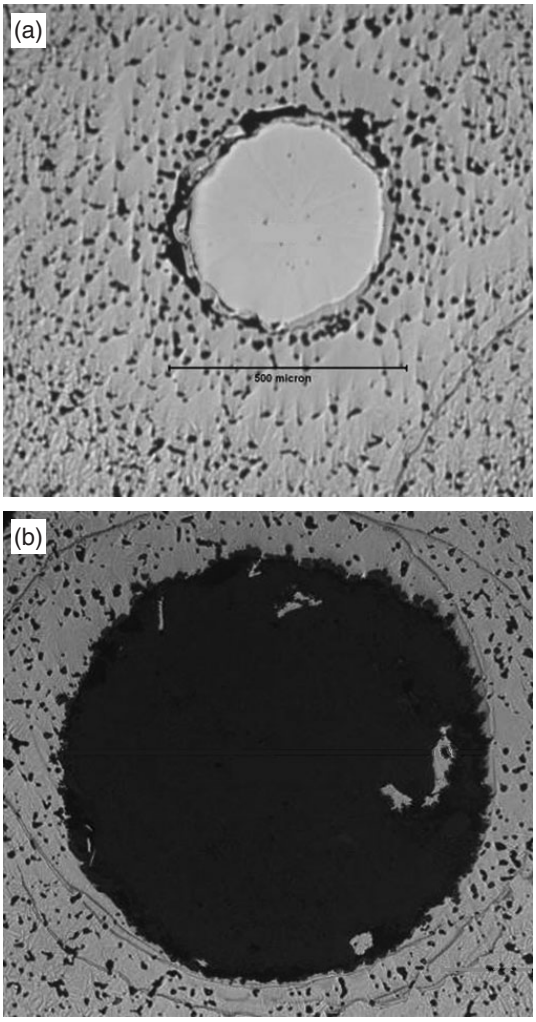

Fig. 5. Radial cross-section of titanium billet containing (a) a 406 μm uncarburized iron wire and (b) a cylindrical cavity with a larger 800 μm diameter produced by dissolution of the wire (polishing debris are embedded in phenolic resin filling the cavity). Both images have the same magnification.

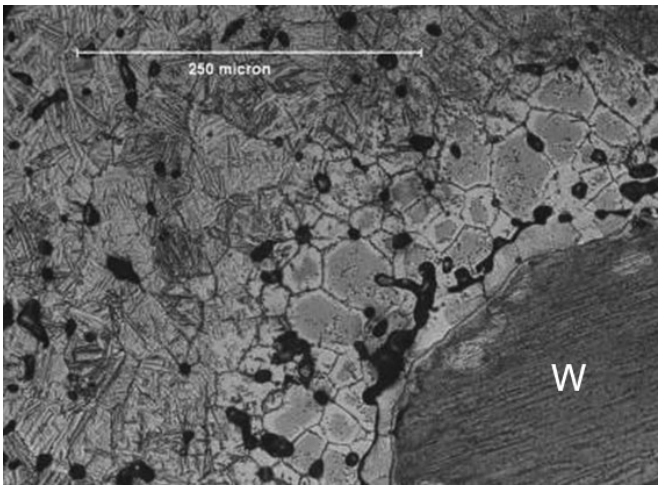

Fig. 6. Radial cross-section of titanium billet, containing a 406 μm uncarburized iron wire (marked "w"), etched with a modified Kroll's etchant to expose the grain microstructure of the titanium matrix, which shows a ~ 150 μm thick shell of coarse grains surrounding the iron wire, expected to correspond to a high Fe diffusion zone.

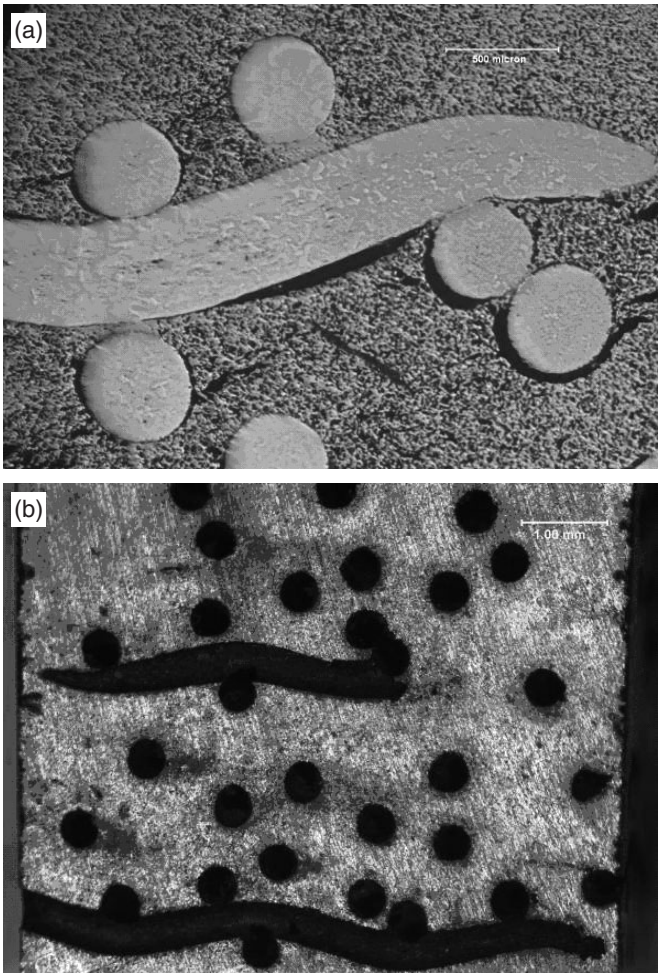

Fig. 7. Cross-section of titanium billet with carburized steel meshes: (a) before dissolution, with woven 508 μm diameter steel wires (b) after dissolution, with interconnected porosity replicating the mesh wires.

the resulting porous titanium after dissolution shown in Figure 7(b) illustrates the elongated and wavy shape of the cavities in two orthogonal directions and the good connectivity between the orthogonal cavity layers. Titanium foams produced by this process may thus display highly elongated pores with constant diameter and good interconnectivity. For bone implant applications, this may encourage bone ingrowth more than in existing titanium foams with equiaxed pores, typically exhibiting narrow fenestrations between pores which may prevent deep penetration of the bone into the foam.[7,19,20]

Spherical Cavities

Figure 8 shows the cross-section of a cavity created by dissolution of a single steel sphere with 1.58 mm diameter (more than three times the diameter of the wire shown in Fig. 4) from the sintered titanium matrix. The sphere shape is faith-

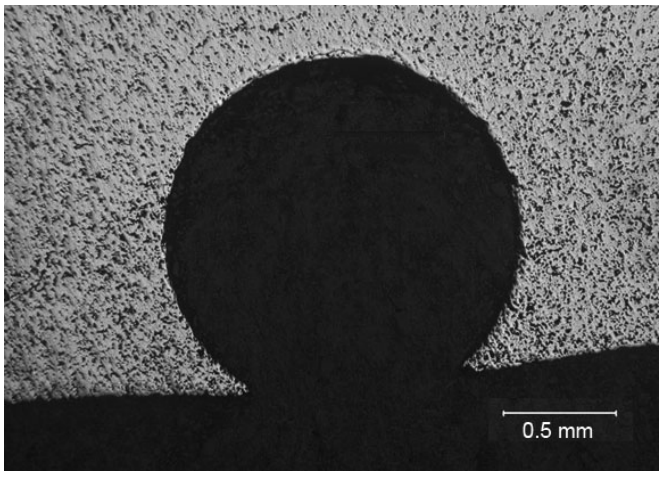

Fig. 8. Cross-section of spherical cavity in sintered titanium produced by dissolution of a 1.58 mm diameter steel sphere.

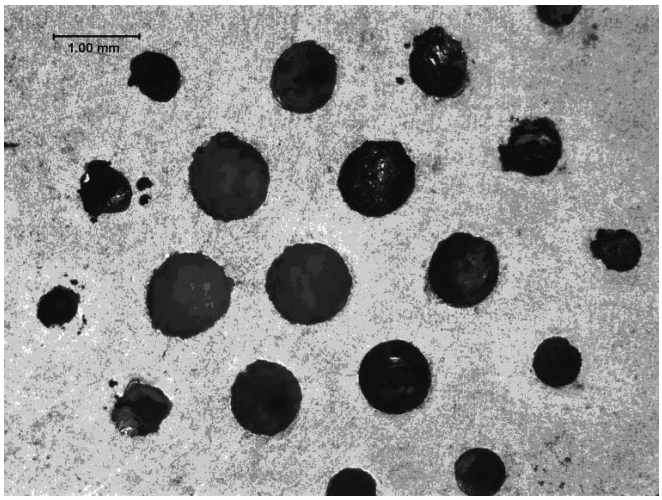

Fig. 10. Micrograph of surface of titanium billet containing a hexagonal array of spherical pores produced by dissolution of 1.58 mm diameter steel spheres placed in a close-packed array.

fully replicated, and the sharp edge near the surface demonstrates that dissolution of the cathodically-protected titanium matrix did not take place, similar to the carbon-containing wires shown in Figures 3–4. This is despite the lower carbon content of the spheres (0.1–0.2 wt.%) as compared to the wires (0.80–0.95 wt.%), indicating that relatively low carbon content are sufficient for TiC formation to prevent interdiffusion between Fe and Ti during the sintering step. No TiC was visible in these and any other cross-sections under optical microscopy, indicating that the layer is very thin, removed during dissolution or possibly abraded during metallographic preparation.

Figures 9 and 10 show that arrays of steel spheres can produce highly porous surfaces, with cavities with well-defined size and reentrant volumes. The latter aspect is particularly useful for mechanical anchorage by bone ingrowth in medical implant. These figures also demonstrate that, even as a single surface layer, the present technique may produce a porous layer with a much more regular geometry and thus better static and fatigue strength than the current porous layers of partially-sintered beads with angular pores used in titanium implants.[19,20] These experiments also illustrate the feasibility of creating three-dimensional open porosity in foams with highly regular spherical porosity and low relative density by stacking planar arrays of steel spheres, filling the interstices with fine titanium powders, sintering the composite and electro-chemically removing the spherical space-holders.

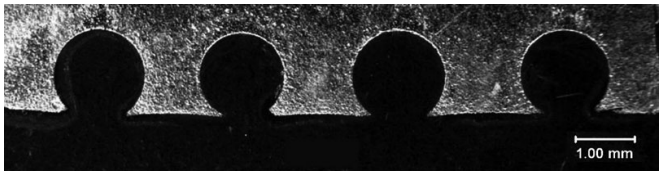

Fig. 9. Cross-section of titanium billet with row of spherical cavities produced by dissolution of 1.58 mm diameter steel spheres.

Outlook

The use of steel as a space-holder to create porosity in titanium has many advantages as compared to the other organic and inorganic space-holders used to date (carbamide, ammonium hydrogen carbonate, water ice or polymer, as reviewed in the introduction). First, hydrogen and oxygen contamination by the spaceholder is completely avoided, which is particularly important for titanium given its propensity for embrittlement by these elements. Second, steel with various geometries (*e.g.*, powders, balls, wires and meshes) is readily available in a variety of sub-millimeter sizes. Third, the surface of the space-holder can be either smooth (*e.g.*, for an as-drawn wire) or irregular (*e.g.*, after partial etching of wires), thus allowing to tailor the surface of the replicated pores. Finally, because the steel phase is nearly incompressible, hydrostatic pressure can be applied during densification (*e.g.*, by hot-isostatic pressing, hot pressing or hot extrusion) to completely densify the titanium phase; this is not possible with the other space-holders that are removed early in the titanium densification process, leaving pores that would collapse under pressure. The above advantages also apply as compared to magnesium as a space-holder, the only other metallic space-holder reported in the literature for titanium.[4] Magnesium is difficult to create in sub-millimeter wires due to its low ductility which also severely limits the creation of meshes and spheres and it may lead to mixed magnesium/titanium-oxide contamination due to the unavoidable presence of MgO on its surface. Finally, we note that the present process using steel as space-holder may be applicable to other titanium-based alloys (*e.g.*, Ti-6Al-4V and NiTi), and other metals that are more noble than steel (inherently or through passivation, as for titanium).

Conclusions

Titanium preforms containing steel space-holders are sintered to create composites. Upon subsequent electrochemical

ADVANCED ENGINEERING MATERIALS

dissolution of the steel under conditions where the titanium is cathodically protected, porosity is created. Here, we demonstrated that steel spheres, wires, and wire meshes can be removed from an unalloyed titanium matrix, allowing the creation of surface or volume porosity with controllable shapes, dimensions, connectivity and surface finish.

Carbon-free iron wires produce, by interdiffusion, a large shell of iron-containing titanium surrounding the wires, which is removed during the electrochemical dissolution step, thus increasing the cavity size. Accurate dissolution of the space-holder can be achieved by using carbon-containing steel space-holders, which form a TiC diffusion barrier preventing interdiffusion with the titanium matrix.

Received: March 11, 2008
Final version: June 28, 2008
Published online: August 27, 2008

[1] D. C. Dunand, *Adv. Eng. Mater.* **2004**, *6*, 369.
[2] M. Bram, C. Stiller, H. P. Buchkremer, D. Stöver, H. Baur, *Adv. Eng. Mater.* **2000**, *2*, 196.
[3] C. F. Li, Z. G. Zhu, T. Liu, *Powder Metall.* **2005**, *48*, 237.
[4] K. R. Wheeler, M. T. Karagianes, K. R. Sump, *Conf. Titanium Alloys in Surgical Implants*, ASTM, Philadelphia, **1983**, 241–254.
[5] Z. Esen, S. Bor, *Scr. Mater.* **2006**, *56*, 341.
[6] C. E. Wen, M. Mabuchi, Y. Yamada, K. Shimojima, Y. Chino, T. Asahina, *Scr. Mater.* **2001**, *45*, 1147.
[7] B. Otsuki, M. Takemoto, S. Fujibayashi, M. Neo, T. Kokubo, T. Nakamura, *Biomaterials* **2006**, *27*, 5892.
[8] T. Imwinkelried, *J. Biomedical Mater. Res.* **2007**, *81A*, 964.
[9] O. Andersen, U. Waag, L. Schneider, *Adv. Eng. Mater.* **2000**, *2*, 192.
[10] G. Rausch, J. Banhart, in *Handbook of Cellul. Met.* Wiley-VCH, **2002**, 21.
[11] M. W. Kearns, P. A. Blenkinsop, A. C. Barber, T. W. Farthing, *Intern. J. Powder Metall.* **1988**, *24*, 59.
[12] N. G. Davis, J. Teisen, C. Schuh, D. C. Dunand, *J. Mater. Res.* **2001**, *16*, 1508.
[13] E. D. Spoerke, N. G. Murray, H. Li, L. C. Brinson, D. C. Dunand, S. I. Stupp, *J. Biomedical Mater. Res.* **2008**, *84A*, 402.
[14] L. Tuchinskiy, R. Loutfy, *Mater. and Process. for Med. Devices*, ASM, **2004**, 377.
[15] Y. Chino, D. C. Dunand, *Acta Mater.* **2007**, *56*, 105.
[16] H. Huang, H. Zhang, L. Zhou, H. Y. Zheng, *J. Micromech. and Microeng.* **2003**, *13*, 8.
[17] T. Momono, T. Enjo, K. Ikeuchi, *ISIJ Int.* **1990**, *30*, 978–984.
[18] E. A. Brandes, G. B. Brook, *Smithells Met. Ref. Book*, Butterworth-Heineman Ltd, Oxford, **1992**.
[19] D. A. Deporter, P. A. Watson, R. M. Pilliar, A. H. Melcher, J. Winslow, T. P. Howley, P. Hansel, C. Maniatopoulos, A. Rodriguez, D. Abdulla, K. Parisien, D. C. Smith, *J. Dental Res.* **1986**, *65*, 1064.
[20] A. J. T. Clemow, A. M. Weinstein, J. J. Klawitter, J. Koeneman, J. Anderson, *J. Biomedical Mater. Res.* **1981**, *15*, 73.

